

# Effect of Extragranular Microcrystalline Cellulose on Compaction, Surface Roughness, and In Vitro Dissolution of a Self-Nanoemulsified Solid Dosage Form of Ubiquinone

Sami Nazzal, Abdel-Azim Zaghloul, and Mansoor A. Khan\*

The authors evaluate the effect of microcrystalline cellulose (MCC) on the tableting performance, surface roughness, and dissolution properties of a dry adsorbed self-nanoemulsified powdered formulation. Heckel analysis was used to study the **tableability, compressibility, and compactibility of six formulas prepared with various MCC grades**. Surface topography revealed a higher degree of waviness at the lower surface of the compacts as the result of granule segregation. The dissolution rate of the nanoemulsion from the tablets increased with increasing MCC particle size. Good flow properties of the formulations resulted from the granular nature of the mixtures. Low hardness and friability indicated oil-induced bridging between the particles.

**Sami Nazzal** is a doctoral student in pharmaceutical sciences, **Abdel-Azim Zaghloul, PhD**, is a postdoctoral research associate, and **Mansoor A. Khan, RPh, PhD**, is a professor of pharmaceutical sciences and the director of the graduate program at the School of Pharmacy at Texas Tech University Health Sciences Center, 1300 Coulter, Amarillo, TX 79106, tel. 806.356.4000, ext. 285, fax. 806.356.4034, khan@ama.ttuhsu.edu.

\*To whom all correspondence should be addressed.

Ubiquinone, also known as Coenzyme Q<sub>10</sub>, is an important component of the mitochondrial respiratory chain (1). Because of its poor aqueous solubility, Coenzyme Q<sub>10</sub> (CoQ<sub>10</sub>) presents a challenge when developing a formulation for oral administration. Many approaches have been used to improve the in vitro dissolution of CoQ<sub>10</sub>. Some of the approaches include complexation with cyclodextrins (2), preparation of redispersible dry emulsion (3), solid dispersion (4), and recently, development of a eutectic-based self-nanoemulsified drug delivery system (5). Self-emulsifying drug delivery systems (SEDDS) are isotropic mixtures of oil, surfactant, cosurfactant, and drug that form a fine oil-in-water emulsion when introduced into an aqueous medium during gentle agitation (6,7).

SEDDS-based formulations, however, require filling into soft or hard gelatin capsules. It was therefore of interest to incorporate the self-emulsifying vehicles into a powder to produce solid dosage forms. Recently, pellets containing a self-emulsifying mixture were prepared by extrusion-spheronization (8). Solid-state microemulsion for the delivery of cyclosporin also was prepared by coating the premicroemulsion with an enteric material (9). Similarly, a solvent-evaporation method was used to prepare tocopheryl nicotinate tablets using calcium silicates as the adsorbing agent (10). Such methods often require elaborate processing and instrumentation.

On the other hand, Jarowski (11,12) and later Spireas (13–15), produced solid solutions and liquisols by blending liquid medications with selected powder excipients to produce free-flowing, readily compressible powders. Such excipients include cellulose or lactose as the carriers and fine silicates as the coating material. Using a similar approach, Akzo Nobel (16) and Cima Labs (17) introduced a solid dosage form based on microemulsion adsorbed onto colloidal silicon dioxide and microcrystalline cellulose. In most cases as well as in the case of liquisols, however, adsorbed oil- or lipid-based formulations form a thin film of oil on the surface of the powder. This film causes particles to adhere and produces a mass that exhibits poor flow and tableting characteristics (13). To improve

flow and compaction properties, oil loading is reduced, or fine particulates such as silicates are added in quantities often exceeding the limits stated by the *Code of Federal Regulation*.

In this study, a different approach was used to produce microemulsion-adsorbed compacts. The eutectic-based self-nanoemulsified drug delivery system of CoQ<sub>10</sub> (5) was found to form a wax-like paste when mixed with small quantities of the copolyvidone Kollidon VA 64. In one study, Kollidon VA 64, a copolymer of vinylpyrrolidone and vinyl acetate, was shown to possess a unique dry-binding capacity (18). Copolyvidone paste ground with a suitable excipient produces granules with good flow properties that are readily available for direct compression. Maltodextrin was found to be a good grinding agent for its solubility, particle size, and acceptable adsorbing properties. When compressed, however, the given mixture of copolyvidone paste and maltodextrin produced soft compacts. Therefore, directly compressible microcrystalline cellulose (MCC) was added at 20% loading.

MCC often is regarded as one of the best excipients for direct compression (19). Extragranular MCC was shown to increase dissolution rates and compressibility of tablets made by high-shear granulation (20). Avicel MCC is available in many grades that differ from each other by their particle size, particle shape, and moisture content (21). The initial size of the particles constituting a powder is an important factor in determining its compaction behavior. For most powdered materials, compaction of the smaller particles results in stronger tablets because of the large surface area available for bonding (22). Many studies have investigated the effects of chemical, physical, and mechanical properties of MCC on compressibility (23–27). However, the effect of the initial particle size of MCC — used to prepare emulsion-adsorbed compacts — on the strength of the tablets has not been adequately addressed. The objectives of this study were to

- evaluate the compaction properties of the microemulsion-adsorbed powdered material with an emphasis on the effect of various Avicel MCC grades on the mechanical properties of the compacts
- study the effect of the adsorbed oily formulation on the surface roughness of the tablets
- evaluate the in vitro dissolution of the self-nanoemulsified formulations from their solid compacts.

## Materials and methods

**Materials.** CoQ<sub>10</sub> was provided by Kyowa Hakko USA (New York, NY). Polyoxyl 35 castor oil (Cremophor EL) and copolyvidone (Kollidon VA 64) were obtained from BASF Corp. (Mount Olive, NJ). Medium-chain mono- and diglycerides (Capmul MCM-C8) were obtained from Abitec Corp. (Janesville, WI). Single-fold lemon oil type C.P. Extra FCC was obtained from Citrus and Allied Essences Ltd. (Floral Park, NY). Maltodextrin with a mean particle diameter of 190 μm and a dextrose equivalent of 12.5 (Glucidex IT 12) was obtained from Roquette America, Inc. (Keokuk, IA). Various grades of microcrystalline cellulose (Avicel) were obtained from FMC Corp. (Newark, DE). Physical properties of the Avicel MCC grades used are shown in Table I. High-performance liquid chromatography (HPLC)–grade

**Table I: Physicochemical properties of the Avicel MCC used in the study.**

Avicel MCC Grade	Average Particle Size (μm)	Moisture Content (%)
Avicel PH-105	20	≤5
Avicel PH-101	50	≤5
Avicel PH-113	50	≤2
Avicel PH-102	90	≤5
Avicel PH-112	90	≤1.5
Avicel PH-200	180	≤5

methanol and *n*-hexane were purchased from VWR Scientific (Minneapolis, MN). All the chemicals were used as received.

### Preparation of the solid-state self-nanoemulsified dosage form.

The eutectic-based self-nanoemulsified drug delivery system (SNEDDS) of CoQ<sub>10</sub> was prepared as follows: CoQ<sub>10</sub> and lemon oil at a ratio of 1:1 were accurately weighed into screw-capped glass vials and melted in a water bath at 37 °C. Cremophor EL and Capmul MCM-C8 were added to the oily mix, each at a final concentration of 26.9% w/w. The resultant emulsion was mixed with a stirring bar until a transparent solution of SNEDDS was obtained. The SNEDDS then was allowed to cool at ambient temperature for 24 h until a viscous paste was obtained. Nanoemulsion-adsorbed granular material was obtained from a mixture of SNEDDS paste, Kollidon VA 64, Glucidex IT 12, and Avicel at a ratio of 0.11:0.13:0.56:0.2, respectively. SNEDDS was mixed initially with Kollidon VA 64 using a mortar and pestle until a semisolid waxy paste was obtained. The mixture then was ground with Glucidex IT 12 in the mortar for 1 min to obtain the dry microemulsion-based granules. Finally, Avicel was added to the granules and blended in a V-blender (Patterson-Kelley Co., E. Stroudsburg, PA) for 5 min. Six formulations were made, each with a different grade of Avicel MCC.

**Carr's flowability index.** The flow properties of the solid-state powdered emulsion were determined by Carr's method (28). Compressibility, angle of repose, angle of spatula, and uniformity coefficient were measured.

The granular powder (10 g) was poured lightly into a 25-mL graduated cylinder. The powder was tapped until no further change in volume was observed. Powder bulk density, ρ<sub>b</sub> (g/cm<sup>3</sup>), was calculated as the weight of the powder divided by its volume before tapping. Powder tapped density, ρ<sub>p</sub> (g/cm<sup>3</sup>), was calculated as the weight of the powder divided by its volume after tapping. The percentage of compressibility was computed from the following equation:

$$\% \text{ compressibility} = 100 \left( \frac{\rho_p - \rho_b}{\rho_p} \right)$$

The angle of repose was measured with a protractor for the heap of granules formed by passing 10 g of the sample through a funnel at a height of 8 cm from the horizontal surface. A steel spatula with a 5 × 7/8 in. blade was inserted to the bottom of the heap and withdrawn vertically. The angle of the heap formed on the spatula was measured as the angle of spatula.

The uniformity coefficient was obtained by sieve analysis of 10 g of the powdered material using a Retsch sieve shaker type

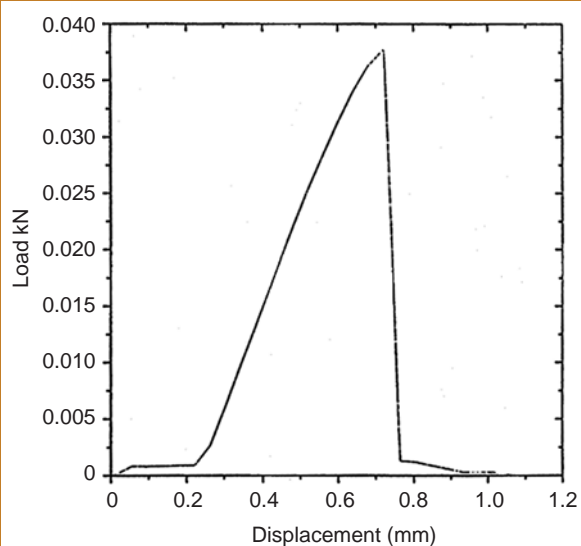


**Figure 1:** A representative load–displacement curve obtained from a three-point flexure test of a self-nanoemulsified tablet dosage form.

AS200 (F. Kurt Retsch GmbH, Germany) fitted with eight US-standard sieves (Dual Mfg. Co., Chicago, IL) ranging in size from 0.075 to 1.7 mm. Uniformity coefficient is the numerical value arrived at by dividing the width of the sieve opening that will pass 60% of the sample by the width of the sieve opening that will pass 10% of the sample. The flowability index was calculated with the point scores, ranging from 0 to 100, in a scale described by Carr to evaluate the flow and the arching properties of powders.

#### Compaction of the solid-state self-nanoemulsified dosage form.

Microemulsion-adsorbed compacts were prepared using concave elongated punches (Natoli Engineering Co., St. Charles, MO). Tablets were made by compressing 1245 mg of the powder, which corresponds to 30 mg in weight of CoQ<sub>10</sub>, between the faces of the punch. Punches were mounted between the platens of a Carver press model C (Carver Inc., Wabash, IN) attached to a semiautomatic compression assembly model 2826 (Carver). The compaction pressure ranged from 15.6 to 312.3 MPa. The dimensions of the compact were measured to  $\pm 0.01$  mm using a dial thickness gauge (Lux Sci. Inst. Corp., New York, NY). Punches were 0.750 in. long and 0.375 in. wide and provided tablets with an area of the curved segment equivalent to 0.0083 in.<sup>2</sup> and a height of the curved surface above the central thickness equivalent to 0.06 in.

**Determination of true density and compact porosity.** The true density,  $\rho_t$ , of the powdered self-emulsified formulation was determined in triplicate using a helium pycnometer, model Ultracycrometer 1000 (Quantachrome, Boynton Beach, FL). The density of the resulting compacts,  $\rho_c$ , was calculated from the weight and volume of the compact. The porosity,  $\epsilon$ , of the compacts was calculated by the following equation:

$$\epsilon = 100 \left( 1 - \frac{\rho_c}{\rho_t} \right)$$

**Determination of tensile strength.** Tensile strength provides a measure of the inherent strength of the compacted material independent of tablet dimensions (29). Tensile strength of the elongated, curve-faced tablets was measured in triplicate with a three-point flexure test using the Instron material-testing instrument model 4442 (Instron Corp., Canton, MA). The load was applied at a rate of 25 mm/min, and the fracture load was obtained from the load–displacement curve recorded using Instron software series IX. A typical load–displacement curve of the microemulsion-based tablets is shown in Figure 1. Tablets were examined for the mode of failure, and only those with the fracture plane running through the center point of the surface of the tablet were used to derive tensile-strength values.

The tensile strength was calculated by the following equation (30,31)

$$\sigma_f = \frac{3FL}{2d^2} \left( \frac{d + 2a}{6A + bd} \right)$$

in which  $\sigma_f$  is the tensile strength;  $F$  is the fracture load in a three-point flexure test;  $b$  and  $d$  are the width and the thickness of the tablet, respectively;  $a$  is the height of the curved surface above the central thickness;  $A$  is the area of the curved segment; and  $L$  is the distance between the lower supports.

**Heckel analysis.** The densification of the dry powdered emulsion was analyzed by the out-of-die Heckel equation (32,33)

$$-Ln \epsilon = KP + D$$

in which  $P$  is the compaction pressure,  $\epsilon$  is the porosity of the compact,  $K$  is the slope of the linear portion of the Heckel plot, and  $D$  is a function of the original compact volume.  $K$  is equal to the reciprocal of the mean yield pressure,  $P_y$ , which is three times the yield strength of the material (34).  $D$  is a constant related to the geometry of the system and the degree of packing of the particles in the die.

**Measurement of surface roughness.** The roughness profiles for the upper and lower surfaces of the compacts were measured with a Mahr perthometer concept 6.3 surface texture-measuring instrument (Mahr Federal Inc., Cincinnati, OH). Tablets were mounted on the X/Y table and scanned with a contact PZK drive unit using the stylus method to move the tracing arm (model MFW-250) across the surface. A tracing length of 3.5 mm was used to obtain 51 profiles with a spacing of 112  $\mu$ m. P-profile, waviness, and roughness parameters were computed for every profile, and the mean of all 51 profiles was collected. The following parameters were measured:

- $P_s$  (profile parameter): the mean distance between local peaks of the P-profile
- $W_s$  (waviness parameter): the mean distance between local peaks of the W-profile
- $R_a$  (roughness average): the arithmetic average of the roughness profile ordinates
- $R_z$  (mean roughness depth of the R-profile): the arithmetic average of roughness depths (i.e., the vertical distance be-

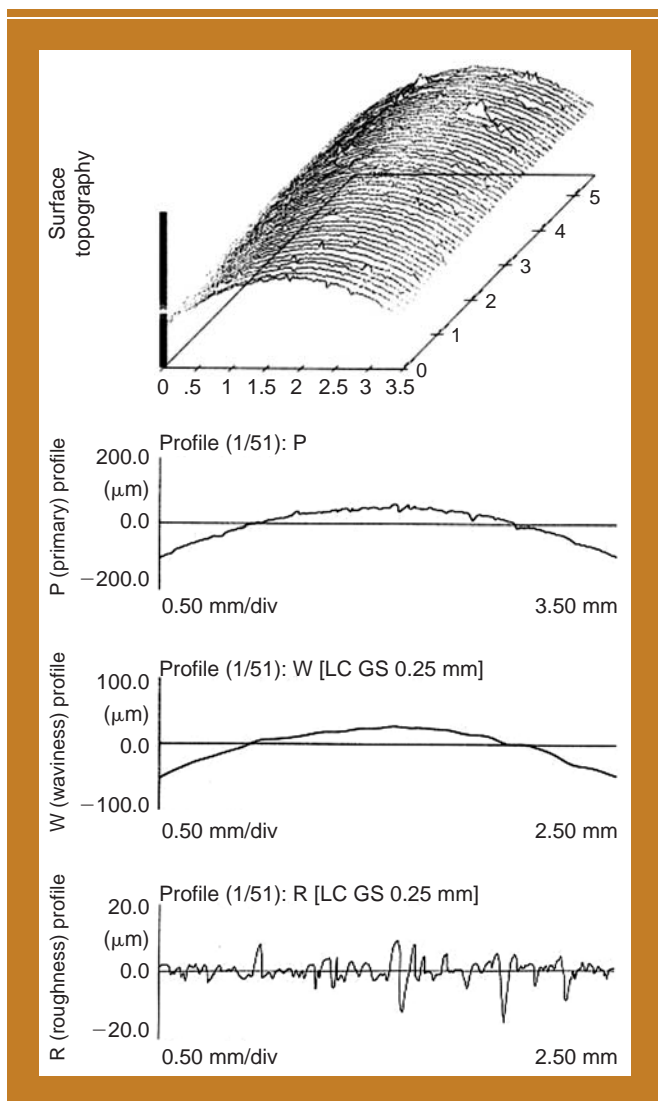


**Figure 2:** A representative surface topography, P, W, and R profiles of self-nanoemulsified tablets, obtained by a Mahr perthometer concept surface-measuring instrument.

tween the highest peak and the deepest valley of consecutive sampling lengths).

- P-profile (primary profile): the mean line generated from the traced profile. Using profile filters, P-profiles separate into long-wave (W-profile) and short-wave (R-profile) compo-

**Table II: Parameters describing disintegration, tableting, and flow properties of formulations made with various Avicel MCC grades.**

Avicel MCC Grade Added to the Formulation	Disintegration Time (min)	Tensile Strength		Yield Strength*		Flowability Index
		$\sigma_0$ (MPa)**	$R^2$ †	(MPa)	$R^2$	
Avicel PH-105	47.82 (0.66)	0.26098	0.987	14.3062	0.994	56.5
Avicel PH-101	30.65 (0.65)	0.35876	0.989	14.368	0.992	63.5
Avicel PH-113	27.88 (1.5)	0.32991	0.997	25.0627	0.948	59
Avicel PH-102	22.775 (1.275)	0.32834	0.991	14.43	0.991	55
Avicel PH-112	23.475 (1.975)	0.38837	0.992	30.8642	0.97	63
Avicel PH-200	15.94 (1.54)	0.34455	0.992	20.202	0.951	52

\*Yield strength calculated from Heckel plot.

\*\*Tensile strength extrapolated to zero porosity.

†Coefficient of determination.

nents. A representative surface topography, P, W, and R profiles obtained by the profilometer are shown in Figure 2.

**Friability and disintegration studies.** The friability of the compacts was measured using a VanKel Type, dual-chamber drum, friability tester (VanKel, Cary, NC) set at a rotation speed of 25 rpm. Five grams of tablets were rotated for 4 min (100 rotations). At the end of the run the tablets were weighed accurately, and the percent friability was computed from the weight of tablets before and after the test. The disintegration time for three replicates was measured using the VanKel single-basket disintegration-testing system at 37 °C according to the *USP XXIV* specification.

**Dissolution studies.** The dissolution profiles of the self-emulsified tablets were determined using a *USP XXIV* rotating basket apparatus (model VK7000, VanKel) at 37 °C. The rotating speed was 50 rpm, and the dissolution medium was 900 mL of water. Samples (3 mL) withdrawn at fixed time intervals were filtered using a 10- $\mu$ m VanKel filter and were assayed for CoQ<sub>10</sub> by HPLC at 275 nm. Briefly, CoQ<sub>10</sub> was analyzed using a C18 3.9  $\times$  150 mm reverse-phase chromatography column (Nova-Pak; Waters, Milford, MA). The mobile phase consisted of methanol-*n*-hexane (9:1) and was pumped at a flow rate of 1.5 mL/min<sup>-1</sup>. The dissolution experiments were conducted in triplicate. Details of the HPLC method can be found elsewhere (35).

## Results and discussion

**Evaluation of flow properties.** One of the limitations of self-emulsified tablet dosage forms is the poor flow of the powdered mass that holds the oily formulation. The flowability index shown in Table II for the microemulsion-adsorbed powdered material was obtained by measuring the powders' mechanical properties (i.e., compressibility, angle of repose, angle of spatula, and uniformity coefficient as previously discussed). According to the method proposed by Carr (28), the flowability performance of a powder with a flow index between 60 and 69 can be described as acceptable. A higher value would indicate a still-better flow, but considering high oil loading in the formulation, the flow values obtained are reasonably good. For direct compression, these values can be improved readily by adding a low concentration of silicates such as silicon dioxide, commonly used as a glidant and anti-adherent. Good flow is the result of the granular nature of

the formulations, which is enhanced primarily by the adsorbing properties of Kollidon VA 64. The effect of MCC particle size on the flow properties of the preparations appeared insignificant.

**Heckel analysis of the powdered self-emulsified formulations.** The Heckel equation is used often to distinguish between the mechanisms of consolidation such as plastic de-

formation and brittle fracture. Three types of Heckel plots were reported that distinguish between the compaction behavior of powdered material on the basis of their particle size or mixture components (36). Data required for Heckel analysis are obtained by either out-of-die or in-die methods. The in-die or at-pressure method collects data during the compaction of the powder. On the other hand, the out-of-die or zero-pressure method requires collecting data after the ejection of the compacts, a procedure that eliminates the effect of elastic deformation on the densification of the powder (37).

The out-of-die Heckel analysis of the compaction of the microemulsion-adsorbed granules containing various grades of MCC is shown in Figure 3. The Heckel plots appear to be linear over the compaction range between 15.6 and 312.3 MPa. Linear regression was performed on the data points of all the powdered materials to calculate the yield strength as previously discussed. Yield strength (see Table II) increased by increasing the particle size of MCC grades having a 5% moisture content. This may be attributed to the effects of the initial particle size on volume reduction. In addition, adsorbing oil onto the surface of the powder may alter its compaction properties.

Several other researchers reported that coating the particles of various pharmaceutical powders with layers of surfactants noticeably alters their mechanical behavior when they are compressed into tablets (38,39). The degree of coating depends on the available surface area and the adsorbing capacity of the powder. Formulations made with Avicel PH-105 had the lowest yield strength at 14.3 MPa (see Table II). This probably is a result of the smaller particle size of Avicel PH-105, which provides a larger surface area for adsorption. This in turn facilitates homogeneous oil distribution throughout the compact, allows efficient particle lubrication and packing, and mediates plastic deformation. Formulations made with Avicel PH-112 and 113 had the highest yield-strength value among the compacts. Avicel PH-112 and 113 have a moisture content of no more than 1.5% and 2% respectively. The reason for the higher yield-strength value is still unclear. It might be the result of moisture-mediated surface adsorption, which limits the formulations' adsorbing capacity. In one reported study, moisture was found to act as a plasticizer and to influence the mechanical properties of MCC (40). Such a phenomenon might help retain surface characteristics and preserve tableting and compaction properties of adjuvants. The adjuvants, Avicel PH-112 and 113, were added merely to boost the compressibility of the soft oil-adsorbed compacts rather than promote oil adsorption.

**Tableting performance of the powdered self-emulsified formulations.** To describe the tableting performance of the powdered microemulsion, compressibility, compactibility, and tabletability of the formulations were evaluated.

**Compressibility.** Compressibility is the ability of a powdered material to undergo a reduction in porosity as a result of applied pressure (22). This could be represented by a plot of porosity against the applied compaction pressure, as shown in Figure 4. Compressibility of the powders is an important factor that governs the strength of compacts, especially at lower compaction pressures. This effect is the result of the formation of a larger interparticulate bonding area and a reduction in porosity that

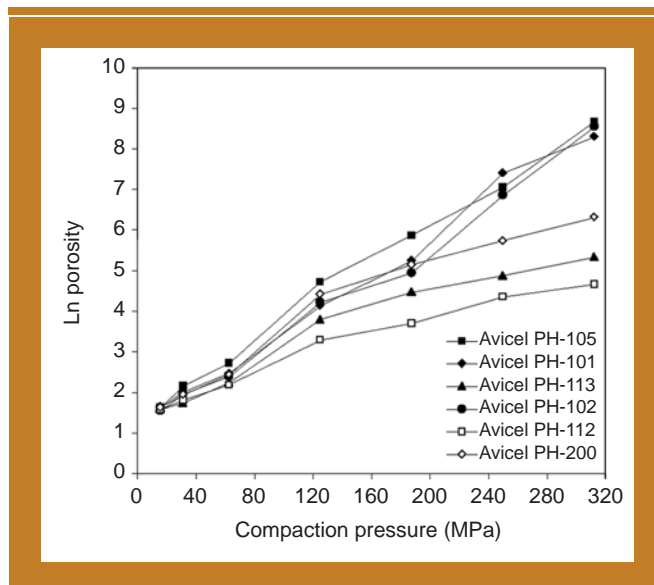


**Figure 3:** Out-of-die Heckel plots of six formulations showing the influence of the added Avicel MCC.

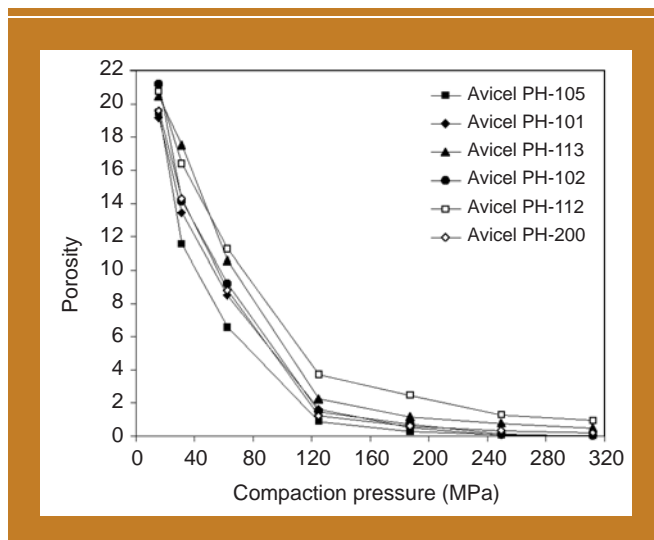


**Figure 4:** Plots of tablet porosity against compaction pressure showing the compressibility of six self-nanoemulsified powdered formulations with various grades of Avicel MCC.

arises from plastic deformation. Hence, the more compressible the powder, the stronger the resultant compacts. When the dry powdered microemulsion-based formulations were compressed under the same compression conditions, compacts made with Avicel PH-105 had the lowest porosity and thus were the most compressible among the adsorbed powders. This result might be attributed to the greater plasticity of the formulation containing Avicel PH-105 as indicated by its low yield strength of 14.3 MPa (see Table II). The outcome also may be the result of the smaller particle size (20  $\mu\text{m}$ ) of Avicel PH-105. Smaller particle size provides larger surface areas for oil adsorption and allows the powder to pack more efficiently. Avicel PH-112 and 113 showed the greatest resistance to plastic deformation at a lower compaction pressure, as observed by their higher yield strengths of 30.9 and 25.1 MPa, respectively (see Table II). Never-

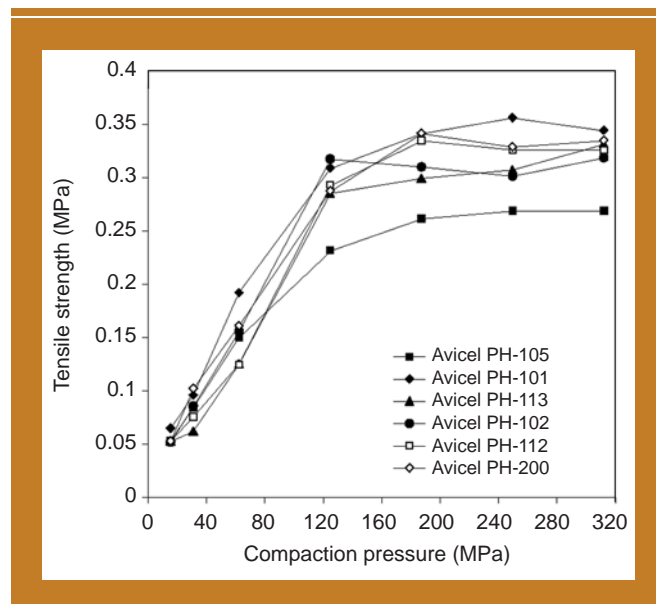
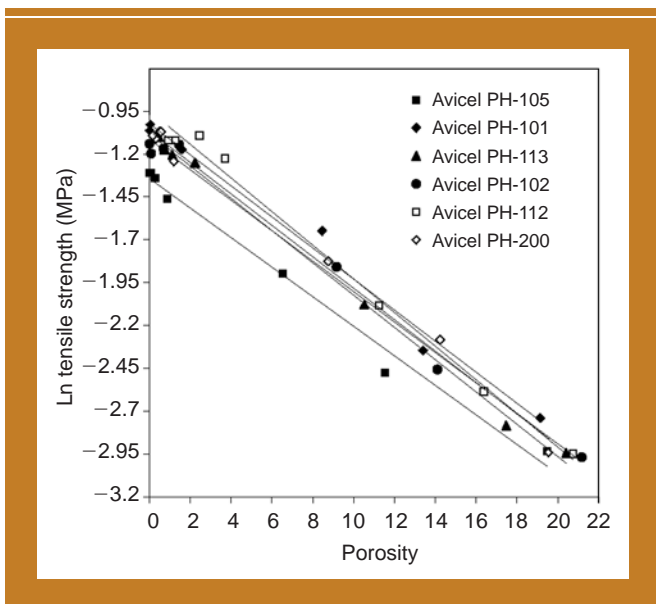


**Figure 5:** Plots of the natural logarithm of tensile strength against porosity showing the compactibility of six self-nanoemulsified powdered formulations with various grades of Avicel MCC.

**Figure 6:** Plots of tensile strength against compaction pressure showing the tableability of six self-nanoemulsified powdered formulations with various grades of Avicel MCC.

theless, all the formulations showed great dependence on compression pressure regardless of MCC particle size. The porosity of all powdered materials decreased rapidly with an increase in compaction pressure  $\leq 120$  MPa and reached relatively constant values thereafter.

**Compactibility.** Compactibility is the ability of a powdered material to produce compacts with sufficient strength under the effect of densification. This can be represented by a plot of tablet tensile strength against the resultant porosity, at which tensile strength decreases exponentially with an increase in porosity (Figure 5). This relationship can be expressed by the following equation (22)

$$\text{Ln}\sigma = \text{Ln}\sigma_0 - b\epsilon$$

in which  $\sigma$  is the tensile strength,  $\sigma_0$  is the tensile strength at zero porosity,  $b$  is a constant related to the pore distribution in the tablets, and  $\epsilon$  is the porosity. Tensile strength at zero porosity,  $\sigma_0$ , was obtained by fitting the equation to the data followed by extrapolation. All powdered formulations followed the exponential relationship described in the equation. Tensile

strength at zero porosity,  $\sigma_0$ , (see Table II) appears independent of the initial MCC particle size. The lowest  $\sigma_0$  value for compacts made with Avicel PH-105 indicates the weakest bonding, which can be attributed to its highest adsorbing capacity. This causes Avicel PH-105 particles to be fully coated with a film of the oily formulation, thereby reducing the ability for interparticulate interactions and surface bonding. Coating lactose particles with poly(ethylene glycol) was reported to minimize the tensile strength of their compacts because wetting and softening the substrates' surfaces prevent the operation of strong substrate-substrate bonds (38).

**Tableability.** Tableability is the ability of a powdered material to produce compacts with sufficient strength under the effect of compaction pressure and is represented by a plot of tablet tensile strength against compression pressure. A linear relationship between tensile strength and compaction pressure was observed for each of the formulations within the compaction range  $< 120$  MPa and reached a plateau thereafter (see Figure 6). The effect of particle size of MCC on tensile strength appears less significant throughout the compaction range. In one study, no difference in hardness was observed in a blend of MCC

**Table III:** P, W, and R surface roughness parameters of the upper and lower surfaces of the tablets as a function of the Avicel MCC grade added to the formulations.

Avicel MCC Grade Added to the Formulation	P-profile		W-profile		R-profile			
	$P_s$ ( $\mu\text{m}$ )		$W_s$ ( $\mu\text{m}$ )		$R_a$ ( $\mu\text{m}$ )		$R_z$ ( $\mu\text{m}$ )	
	Upper	Lower	Upper	Lower	Upper	Lower	Upper	Lower
Avicel PH-105	118.2	151.68	391.02	446.9	2.97	1.83	20.07	12.84
Avicel PH-101	123.82	157.09	373.9	486.62	1.84	1.63	12.92	11.6
Avicel PH-113	143.6	144.24	384.26	427.14	1.96	1.84	14.26	13.08
Avicel PH-102	156.78	173.51	386.88	469.76	1.48	1.31	10.62	9.26
Avicel PH-112	152.31	160.58	357.12	405.87	1.85	1.59	13.53	10.91
Avicel PH-200	162.34	175.16	387.62	431.95	1.77	1.52	12.57	11.04

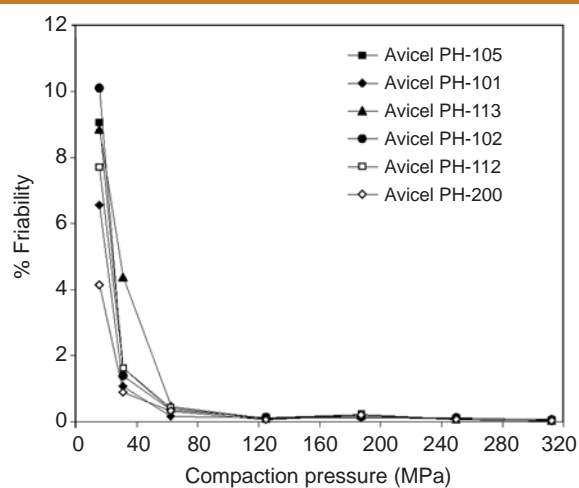


**Figure 7:** Plots of percent friability against compaction pressure of six self-nanoemulsified powdered formulations with various grades of Avicel MCC.

and lactose as a result of MCC particle size (41). Similarly, MCC characteristics such as particle size and size distribution were found to have little effect on the tensile strength of tablets made from spray-dried Avicel (42). This could result from the low MCC loading of 20% in the formulation. The adsorbing capacity of MCC appeared insignificant in terms of producing compacts with distinctive tensile strengths at lower compaction pressures. At compression loads >120 MPa, during which most of the pores are eliminated, the difference in the interparticulate bonding area would be small. At a higher compression pressure, the bonding strength per unit bonding area would be the decisive factor in controlling compact strength. Consequently, Avicel PH-101, 112, and 200 showed the greater tensile strengths of 0.36, 0.39, and 0.34, respectively, at compaction pressures >120 MPa.

**Surface roughness study.** The profile parameters measured for the compacts are listed in Table III. Waviness of the lower surface of the tablets, exposed to the lower punch during compaction, was greater than that of the upper surface of the compacts. This is apparent from the W and P profiles given as  $W_s$  and  $P_s$  parameters, respectively. Higher values of the  $W_s$  parameter for the lower surface of the tablets might be the result of the segregation of the larger granules to the bottom of the die during powder filling. These granules are the Kollidon VA 64-based paste ground with maltodextrin. Segregation was visually evident by the higher degree of mottling of the lower surface caused by the colored granules when compared with the extragranular white MCC powder. However, no change in surface waviness was observed as a function of the initial MCC particle size.

On the other hand, the P-profile measures both roughness and waviness of the surface. Both granule segregation and MCC particle size induced the  $P_s$  parameter, which is a measure of the distance between grooves primarily caused by granules of variable sizes. Higher  $P_s$  values of the lower surface of the compacts indicate that surface waviness is the dominant factor in determining the  $P_s$  parameter.  $P_s$  increased with an increase in

particle size from Avicel PH-105 to Avicel PH-200. This is probably because larger-size MCC provides greater spacing between the particles. Because of powder segregation, the lower punch is exposed to a larger portion of the granules that contain the lipid-based formulation. This in turn provides lubrication to the surface of the punch during tablet compaction and ejection. As a consequence, the roughness profile of the lower surface of the compacts given as  $R_a$  and  $R_z$  was lower than that of the upper surface of the tablets exposed to the less-lubricated upper punch. However, the MCC particle size was less significant in terms of the roughness parameters. This outcome is attributable to the fact that  $R_a$  and  $R_z$  are measures of the heights and depths of the peaks and valleys formed on the surface of the tablets as a result of powder compaction. Plastic deformation might have diminished the differences between MCC particles when they were monitored vertically yet maintained their characteristic boundaries detected by the P-profile parameters.

**Friability study.** Friability of the compacts made from the powdered self-emulsified system as a function of compaction pressure is shown in Figure 7. Friability decreased gradually with an increase in compression load and reached a plateau of <0.1% at compression pressures >120 MPa independent of the initial MCC particle size. This correlates well with the compressibility and tableability data. Porosities and tensile strengths for all the preparations reached their optimum values at 120 MPa, reflecting the greatest interparticulate bonding that was further induced by oil bridging the particles. In a similar observation, increasing the polysorbate 80 concentration in a mixture with sulphanimide and starch was reported to decrease the friability of the granules as well as their hardness (43). This was attributed to the stickiness and aggregation of the fine particles induced by polysorbate 80.

**Dissolution study.** To evaluate the emulsion release from the adsorbing compacts, dissolution studies were performed for tablets prepared at a low compaction pressure of 31.2 MPa. Ideally, SNEDDS should be released from the tablets and completely emulsify into the dissolution medium. This effect was evaluated by measuring the cumulative percent of the drug solubilized into the aqueous medium as part of the released emulsion. Dissolution plots of the self-emulsified tablets are shown in Figure 8. The dissolution rate within the first 45 min appeared to be dependent on MCC particle size. The cumulative percent of CoQ<sub>10</sub> solubilized in 45 min for compacts made with Avicel PH-200, 102, 112, 113, 101, and 105 was 51.5, 49, 44, 39.5, 36, and 8.7%, respectively. After 1 h, dissolution reached a plateau with an average release of 55% (except for Avicel PH-105). Poor CoQ<sub>10</sub> dissolution might be the result of an irreversible hydrophobic interaction between CoQ<sub>10</sub> and MCC. Initial powder compaction and slow disintegration (see Table II) also might have induced irreversible surface adsorption to the soluble excipients of the formulation. This process causes variable release rates. Oily components of the formulation are emulsified into the aqueous medium at a faster rate compared with the release of CoQ<sub>10</sub>. However, tablets made with Avicel PH-105 induced sustained release of CoQ<sub>10</sub> in a time span of 6 h. Similarly, a slower dissolution rate of compacts made with Avicel PH-105 was reported in the literature (44). As previously discussed,

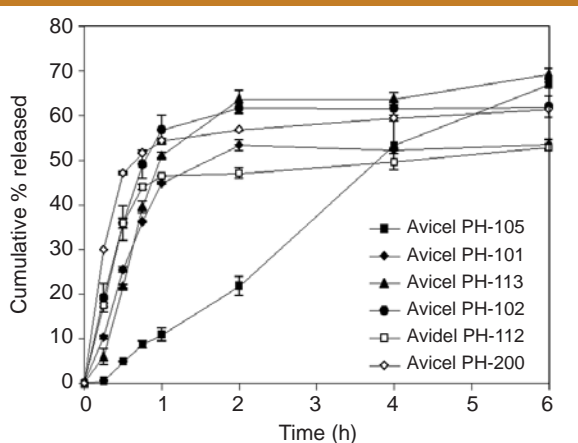


**Figure 8:** Dissolution plots showing the cumulative percent of Coenzyme Q10 released with time from six self-nanoemulsified tablet formulations with various grades of Avicel MCC.

tablets made with Avicel PH-105 had the least yield and tensile strength and the lengthiest disintegration time (see Table II). This suggests oil-induced bridging and sticking between the Avicel particles, an outcome that provides a greater area of contact. The increase in the cohesion between the particles accounts for delayed release rates without increasing the hardness of the tablets. Further studies are required to determine the exact nature of the interactions.

## Conclusion

Powdered self-emulsified dosage forms provide an attractive alternative to filled-capsule preparations. The proper excipient selection, however, is crucial when formulating dry adsorbed solid formulations. Various MCC grades with different particle size and moisture contents vary in their adsorbing capacity. Although an MCC with a smaller particle size such as Avicel PH-105 provides a greater surface area for oil adsorption, it showed a reduction in compactibility and tensile strength. On the other hand, Avicel PH-112, which has larger particles and reduced adsorbing capacity, demonstrated improved hardness and compaction. This was evident from Heckel plots that correlated porosity with tensile strengths and compaction pressure.

Good flow properties of the formulas are the result of the granular nature of the powdered mixture and the unique adsorbing properties of SNEDDS on Kollidon VA 64. No effect of MCC grade and size was evident in terms of the friability of the compacts. Greater waviness of the lower surface of the tablets resulted from the segregation of the granules during die filling. The effect of MCC particle size was evident on the  $P_s$  profile parameter. However, this effect was negligible when evaluated using the R-profile parameters. The dissolution rate of the self-emulsified formulations from the compacts increased, and their disintegration time decreased with an increase in MCC particle size. For most of the preparations, complete release was observed within the first hours, except for the formulation made with Avicel PH-105 that showed a sustained-release effect.

## Acknowledgments

Part of this work was supported by the Texas ATP/ARP grant, 010674-0110-1999. The authors wish to thank Dr. Quentin Smith and Dean Arthur Nelson for their support in establishing the Center for Drug Delivery and Formulations at Texas Tech University School of Pharmacy. Appreciation also is extended to Dr. Indra K. Reddy for his invaluable help. The authors also are grateful to Mr. Don Weirick of Quantachrome Corp. for helping with the true-density measurements.

## References

- G. Grossiet al., "Improved High-Performance Liquid Chromatographic Method for the Determination of Coenzyme Q<sub>10</sub> in Plasma," *J. Chromatogr.* **593**, 217–226 (1992).
- A. Lutka and J. Pawlaczyk, "Inclusion Complexation of Coenzyme Q<sub>10</sub> with Cyclodextrins," *Acta. Polon. Pharm.* **52** (5), 379–386 (1995).
- H. Takeuchi et al., "Improvement of Photostability of Ubidecarenone in the Formulation of Novel Powdered Dosage Form Termed Redispersible Dry Emulsion," *Int. J. Pharm.* **86**, 25–33 (1992).
- S. Nazzal et al., "Preparation and Characterization of Coenzyme Q<sub>10</sub> — Eudragit Solid Dispersion," *Drug. Dev. Ind. Pharm.* **28** (1), 49–57 (2002).
- S. Nazzal et al., "Preparation and In Vitro Characterization of a Eutectic-Based Semisolid Self-Nanoemulsified Drug Delivery System (SNEDDS) of Ubiquinone: Mechanism and Progress of Emulsion Formation," *Int. J. Pharm.* **235**, 247–265 (2002).
- S.A. Charman et al., "Self-Emulsifying Drug Delivery Systems: Formulation and Biopharmaceutical Evaluation of an Investigational Lipophilic Compound," *Pharm. Res.* **9** (1), 87–93 (1992).
- D.Q.M. Craig et al., "An Investigation into the Physico-Chemical Properties of Self-Emulsifying Systems Using Low-Frequency Dielectric Spectroscopy, Surface-Tension Measurements, and Particle-Size Analysis," *Int. J. Pharm.* **96**, 147–155 (1993).
- M. Newton et al., "The Influence of Formulation Variables on the Properties of Pellets Containing a Self-Emulsifying Mixture," *J. Pharm. Sci.* **90** (8), 987–995 (2001).
- C. Kim et al., "Once-a-Day Oral Dosing Regimen of Cyclosporin A: Combined Therapy of Cyclosporin A Premicroemulsion Concentrates and Enteric Coated Solid-State Premicroemulsion Concentrates," *Pharm. Res.* **18** (4), 454–459 (2001).
- Y. Takashima et al., "Reduction of Tablet Coloration at Tableting for Oily Medicine (Tocopheryl Nicotinate)," *Int. J. Pharm.* **187**, 125–135 (1999).
- K.Y. Yang, R. Glemza, and C.I. Jarowski, "Effect of Amorphous Silicon Dioxide on Drug Dissolution," *J. Pharm. Sci.* **68** (5), 560–565 (1979).
- C. Liao and C.I. Jarowski, "Dissolution Rates of Corticoid Solutions Dispersed on Silicas," *J. Pharm. Sci.* **73** (3), 401–403 (1984).
- S.S. Spireas, C.I. Jarowski, and B.D. Rohera, "Powdered Solution Technology: Principles and Mechanism," *Pharm. Res.* **9** (10), 1351–1358 (1992).
- S. Spireas and S. Sadu, "Enhancement of Prednisolone Dissolution Properties Using Lquisolid Compacts," *Int. J. Pharm.* **166**, 177–188 (1998).
- S. Spireas, S. Sadu, and R. Grover, "In Vitro Release Evaluation of Hydrocortisone Lquisolid Tablets," *J. Pharm. Sci.* **87** (7), 867–872 (1998).
- P. de Haan and H.G.M. Poels-Janssen, "Solid Pharmaceutical Composition Comprising an Excipient Capable of Binding Water," United States Patent No. 6,187,339 (2001).
- S.I. Pather et al., "Microemulsion as Solid Dosage Forms for Oral Administration," United States Patent No. 6,280,770 (2001).
- K. Kolter and D. Flick, "Structure and Dry Binding Activity of Different Polymers, Including Kollidon VA 64," *Drug. Dev. Ind. Pharm.* **26** (11), 1159–1165 (2000).
- E. Lahdenpaa, M. Niskanen, and J. Yliruusi, "Crushing Strength, Disintegration Time, and Weight Variation of Tablets Compressed from Three Avicel PH Grades and Their Mixtures," *Eur. J. Pharm. Biopharm.* **43**, 315–322 (1997).



20. J.Z. Li et al., "The Role of Intra- and Extragranular Microcrystalline Cellulose in Tablet Dissolution," *Pharm. Dev. Tech.* **1** (4), 343–355 (1996).
21. Avicel Technical Literature, FMC Corporation, Philadelphia, PA (1998).
22. C. Sun and D.J.W. Grant, "Effect of Initial Particle Size on the Tableting Properties of L-Lysine Monohydrochloride Dihydrate Powder," *Int. J. Pharm.* **215**, 221–228 (2001).
23. T. Tsai et al., "Modification of Physical Characteristics of Microcrystalline Cellulose by Codrying with *b*-Cyclodextrins," *J. Pharm. Sci.* **87** (1), 117–122 (1998).
24. K. Obae, H. Iijima, and K. Imada, "Morphological Effect of Microcrystalline Cellulose Particles on Tablet Tensile Strength," *Int. J. Pharm.* **182**, 155–164 (1999).
25. R. Hwang and G.R. Peck, "A Systematic Evaluation of the Compression and Tablet Characteristics of Various Types of Microcrystalline Cellulose," *Pharm. Technol.* **25** (3), 112–132 (2001).
26. P.W.S. Heng and O.M.Y. Koo, "A Study of the Effect of the Physical Characteristics of Microcrystalline Cellulose on Performance in Extrusion Spheronization," *Pharm. Res.* **18** (4), 480–487 (2001).
27. S. Edge et al., "Directional Bonding in Compacted Microcrystalline Cellulose," *Drug. Dev. Ind. Pharm.* **27** (7), 613–621 (2001).
28. R.L. Carr, "Evaluating Flow Properties of Solids," *Chem. Eng.* **18** (1), 163–168 (1965).
29. S.T. David and L.L. Augsburg, "Flexure Test for Determination of Tablet Tensile Strength," *J. Pharm. Sci.* **63** (6), 933–936 (1974).
30. P. Stanley and J.M. Newton, "The Tensile Fracture Stress of Capsule-Shaped Tablets," *J. Pharm. Pharmac.* **32** (12), 852–854 (1980).
31. J.M. Newton, I. Haririan, and F. Podczek, "The Determination of the Mechanical Properties of Elongated Tablets of Varying Cross Section," *Eur. J. Pharm. Biopharm.* **49**, 59–64 (2000).
32. R.W. Heckel, "Density–Pressure Relationship in Powder Compaction," *Trans. Metall. Soc. AIME* **221**, 671–675 (1961).
33. R.W. Heckel, "An Analysis of Powder-Compaction Phenomena," *Trans. Metall. Soc. AIME* **221**, 1001–1008 (1961).
34. C. Sun and D.J.W. Grant, "Compaction Properties of L-Lysine Salts," *Pharm. Res.* **18** (3), 281–286 (2001).
35. S. Nazzari et al., "Analysis of Ubidecarenone (CoQ<sub>10</sub>) Aqueous Samples Using Reversed-Phase Liquid Chromatography," *Die Pharmazie* **56** (5), 394–396 (2001).
36. J.A. Hersey, "Powder Consolidation during Pharmaceutical Tableting," *Drug. Dev. Ind. Pharm.* **1** (3), 223–229 (1974).
37. C. Sun and D.J.W. Grant, "Influence of Elastic Deformation of Particles on Heckel Analysis," *Pharm. Dev. Tech.* **6** (2), 193–200 (2001).
38. S. Malamataris and N. Pilpel, "Tensile Strength and Compression of Coated Pharmaceutical Powders: Tablets," *J. Pharm. Pharmac.* **35**, 1–6 (1983).
39. N. Pilpel, C.I. Igwilo, and S. Malamataris, "Effects of Molecular Coatings on the Compression and Tableting of Some Pharmaceutical Powders," *Int. J. Pharm.* **68**, 157–166 (1991).
40. G.E. Amidon and M.E. Houghton, "Effect of Moisture on the Mechanical and Powder-Flow Properties of Microcrystalline Cellulose," *Pharm. Res.* **12** (6), 923–929 (1995).
41. N.K. Patel et al., "Evaluation of Microcrystalline Cellulose and Lactose Excipients Using an Instrumented Single-Station Tablet Press," *Int. J. Pharm.* **110**, 203–210 (1994).
42. A. McKenna and D.F. McCafferty, "Effect of Particle Size on the Compaction Mechanism and Tensile Strength of Tablets," *J. Pharm. Pharmac.* **34**, 347–351 (1982).
43. P.W.S. Heng and L.S.C. Wan, "Physical Properties of Granules Containing Polysorbate 80," *Drug. Dev. Ind. Pharm.* **13** (2), 355–367 (1987).
44. D. Sixsmith, "Effect of Compression on Some Physical Properties of Microcrystalline Cellulose Powders," *J. Pharm. Pharmac.* **29** (1), 33–36 (1977). **PT**